Electronic Supporting Information

Novel dopant-free hole transport materials enabling 20.9% efficiency perovskite solar cells

Xinxing Yin,[a] Jiaxing Song,[a] Lin Hu,[a] Yingzhi Jin,[a] Lei Lu,[b] Zhen Su[a] and Zaifang Li*[a]*

Dr. Xinxing Yin, Dr. Jiaxing Song, Dr. Lin Hu, Dr. Yingzhi Jin, Dr. Zhen Su, Prof. Zaifang Li
China-Australia Institute for Advanced Materials and Manufacturing (IAMM), Jiaxing University, Jiaxing 314001, China.
E-mails: xxyin@zjxu.edu.cn; zaifang.li@zjxu.edu.cn

Dr. Lei Lu
College of Biological, Chemical Science and Chemical Engineering, Jiaxing University, Jiaxing 314001, China.

*Corresponding Authors

Contents

1. Experimental section

^{1}H and ^{13}C NMR spectra were recorded with Bruker Avance III 500 (500 MHz) spectrometer at room temperature. Mass spectra were obtained by Bruker ultrafleXtreme MALDITOF/TOF. The absorption spectra were measured on a UV-Vis spectrophotometer (Cary 5000, Agilent). The electrochemical cyclic voltammetry (CV) was conducted on an electrochemical workstation (CHI660D Chenhua, Shanghai) with Pt plate as working electrode, Pt slice as counter electrode, and Ag/AgCl electrode as reference electrode in tetrabutylammonium hexafluorophosphate (n-Bu_4NPF_6, 0.1 M) acetonitrile solutions at a scan rate of 50 mV s^{-1}. HTM films are coated on Pt plate electrode for CV, they keep solid film state during the test. Ferrocene/ferrocenium (Fc/Fc^+) was used as the internal standard (the energy level of Fc/Fc^+ is -4.8 eV under vacuum). The HOMO energy level was determined from the calibrated onset oxidation (E_{onset}^{ox}) as HOMO = -4.8-E_{onset}^{ox} (eV); while the LUMO energy level was calculated with HOMO and optical bandgap (E_g) by the formula as: LUMO = HOMO + E_g (eV). Thermogravimetric analysis (TGA) was conducted under N_2 atmosphere at a heating rate of 20 ℃ min^{-1} from 50 ℃ to 800 ℃. The instrument type was SAT-409PC (NETZSH). DSC was conducted on DSC-200PC (NETZSH) at a scan rate of 10 ℃ min^{-1} from 50 ℃ to 250 ℃. The UPS spectra were performed using HeI 21.22 eV as exciting source with energy resolution of 50 meV. Work function was derived from the secondary electron cut-off and the ionization potential from the frontier edge of the occupied density of states. The spectra were calibrated by referencing to the Fermi level of the Ar^+ ion sputter-clean Au substrate. The thickness of films were measured from the stylus profiler (Dektak XT, Bruker).

All calculations were performed using Density Functional Theory (DFT) established in Gaussian16 code. The hybrid functional B3LYP/6-31g (d, p) was used for basic optimization and B3LYP/6-311g (d, p) was used for further electrostatic surface potential simulation.

TRPL measurements were conducted similarly as described in our earlier works.[1] PL decay curves were biexponential in nature and fitted by iterative re-convolution with the measured system response function. Mean photogenerated carrier lifetimes for the biexponential fit are calculated by the weighted average method. *J-V* curves were measured in air under 100 mW cm^{-2} AM1.5G solar irradiation (Enli technology co., ltd) with a Keithley 2400 Source Meter. The incident light was controlled by a shutter. The steady-state efficiencies were obtained by tracking the maximum output power point.

EQE spectra were performed on a QE system (QE-R, Enli technology co., ltd) using 100 Hz chopped monochromatic light ranging from 300 to 850 nm under near-dark test conditions. All characterizations and measurements were performed in the ambient.

Hole-only devices with the configuration of ITO/PEDOT:PSS/HTM/Au were used to evaluate charge mobilities by space charge-limited currents (SCLC) model. We didn't do any thermal annealing to HTM films during SCLC test since HTMs used in PSCs were not annealed. The thickness of HTM was around 100 nm. The thickness of films was measured from the stylus profiler (Dektak XT, Bruker) with a vertical resolution of 1 Å. We first measured the thickness of PEDOT:PSS and determined the thickness of HTM films by the average of 5 test results. The charge mobilities were determined by fitting the dark current according to the following equation:

$$J(V) = \frac{9V^2}{8L^3}\varepsilon_0\varepsilon_r\mu_0 e^{(0.89\gamma\sqrt{V/L})}$$

Where J is the dark current density (mA cm^{-2}), μ_0 is the zero-field mobility (cm^2 V^{-1} s^{-1}), ε_0 is the permittivity of free space, ε_r is the relative permittivity of the material, V is the effective voltage ($V = V_{\text{Applied}} - V_{\text{Built-in}} - V_{\text{series resistane}}$), and L is the thickness of the active layer.

2. Synthesis

Commercially available reagents were purchased from Energy or Admas and used without further purification. Toluene and tetrahydrofuran (THF) were freshly distilled before use. Other solvents were used directly.

Synthesis of BDD-T

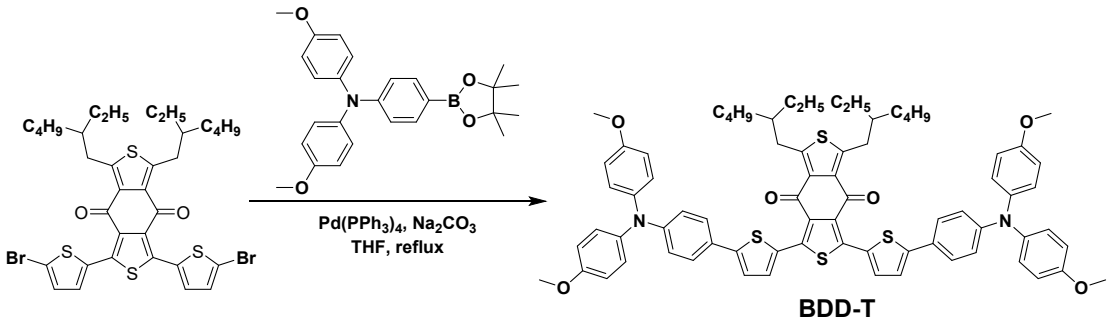

Scheme S1. Synthetic route of **BDD-T**

BDD-T

1,3-Bis(5-bromothiophen-2-yl)-5,7-bis(2-ethylhexyl)benzo[1,2-c:4,5-c′]dithiophene-4,8-dione and 4-methoxy-N-(4-methoxyphenyl)-N-(4-(4,4,5,5-tetramethyl-1,3,2-dioxaborolan-2-yl)phenyl)aniline were synthesized according to literatures.[2, 3]

1,3-Bis(5-bromothiophen-2-yl)-5,7-bis(2-ethylhexyl)benzo[1,2-c:4,5-c′]dithiophene-4,8-dione (0.30 g, 0.39 mmol), 4-methoxy-N-(4-methoxyphenyl)-N-(4-(4,4,5,5-tetramethyl-1,3,2-dioxaborolan-2-yl)phenyl)aniline (0.51 g, 1.17 mmol) and $Pd(PPh_3)_4$ (45 mg, 0.04 mmol) were placed in a round-bottomed flask. THF (20 mL, degassed with nitrogen) and Na_2CO_3 solution (3.9 mL, 2.0 M, degassed with nitrogen) were added. The mixture was refluxed for 48 h. After cooling to room temperature, the mixed solution was extracted with CH_2Cl_2, washed with water, dried and evaporated under vacuum. **BDD-T** (0.48 g, 82%) was obtained by column chromatography on silica gel using petroleum ether/ethyl acetate, 5:1, v/v. ^{1}H NMR (500 MHz, $CDCl_3$, δ): 7.78 (d, *J* = 4.0 Hz, 2H), 7.47 (d, *J* = 8.6 Hz, 4H), 7.18 (s, 2H), 7.14 – 7.04 (m, 8H), 6.92 (d, *J* = 8.7 Hz, 4H), 6.90 – 6.80 (m, 8H), 3.81 (s, 12H), 3.33 (d, *J* = 7.1 Hz, 4H), 1.77 (s, 2H), 1.44 – 1.26 (m, 16H), 0.90 (m, 12H). ^{13}C NMR (125 MHz, $CDCl_3$, δ): 177.70, 156.14, 153.02, 148.74, 148.27, 142.31, 140.47, 133.19, 132.00, 131.84, 131.45, 126.84, 126.70, 125.82, 122.00, 120.14, 114.78, 55.49, 41.22, 33.64, 32.81, 28.87, 26.03, 23.03, 14.14, 10.90. MALDI-TOF MS: m/z=1214.4415 $[M]^+$, calcd. for $C_{74}H_{74}N_2O_6S_4$: 1214.4430. Elemental analysis: calcd. for $C_{74}H_{74}N_2O_6S_4$: C 73.11, H 6.14, N 2.30, S 10.55; found: C 72.68, H 6.03, N 1.82, S 11.07.

Synthesis of BTT-T

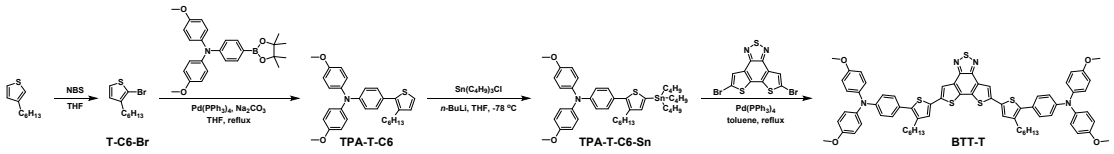

Scheme S2. Synthetic route of **BTT-T**

T-C6-Br

3-Hexylthiophene (5.00 g, 29.71 mmol) was dissolved in 50 mL THF. N-Bromosuccinimide (5.29 g, 29.71 mmol) was added in portions in dark at 0 ℃. The mixed solution was stirred overnight and quenched with water. The crude mixture was extracted with CH_2Cl_2, washed with water, the combined organic phase was dried over by $MgSO_4$ and concentrated in vacuo. The residue was purified by column chromatography (petroleum ether) to afford **T-C6-Br** as colorless oil (7.00 g, 95%).

^{1}H NMR (500 MHz, $CDCl_3$, δ): 7.18 (d, *J* = 5.4 Hz, 1H), 6.80 (d, *J* = 5.4 Hz, 1H), 2.56 (ddt, *J* = 8.4, 5.3, 2.6 Hz, 2H), 1.41 – 1.16 (m, 8H), 0.98 – 0.77 (m, 3H).

TPA-T-C6

T-C6-Br (2.39 g, 9.69 mmol), 4-methoxy-N-(4-methoxyphenyl)-N-(4-(5-(tributylstannyl)thiophen-2-yl)phenyl)aniline (3.50 g, 8.07 mmol) and $Pd(PPh_3)_4$ (19 mg, 0.02 mmol) and $Pd(PPh_3)_4$ (932.90 mg, 0.81 mmol) were placed in a round-bottomed flask. THF (100 mL, degassed with nitrogen) and Na_2CO_3 solution (26.9 mL, 3.0 M, degassed with nitrogen) were added. The mixture was refluxed for 48 h. After cooling to room temperature, the mixed solution was extracted with CH_2Cl_2, washed with water, dried and evaporated under vacuum. **TPA-T-C6** (3.10 g, 81%) was obtained by column chromatography on silica gel using petroleum ether/ethyl acetate, 20:1, v/v. ^{1}H NMR (500 MHz, $CDCl_3$, δ): 7.23 (s, 2H), 7.10 (t, *J* = 17.4 Hz, 5H), 6.95 (d, *J* = 5.2 Hz, 2H), 6.85 (d, *J* = 8.3 Hz, 5H), 3.81 (s, 6H), 2.64 (s, 2H), 1.37 – 1.21 (m, 8H), 0.96 – 0.73 (m, 3H).

TPA-T-C6-Sn

To a solution of **TPA-T-C6** (1.00 g, 2.12 mmol) in 30 mL dry THF cooled at -78 ℃ was added dropwise with n-butyllithium (2.5 M in hexanes, 1.02 mL, 2.54 mmol) under N_2. After complete addition, the reaction was stirred at -78 ℃ for 1 h. After warming to room temperature, the solution was stirred for another 1 h, and then cooled again to -78 ℃, tributyltin chloride (0.83 g, 2.54 mmol) was added. The mixture was warmed to room temperature and stirred overnight. The reaction mixture was quenched with water and extracted with CH_2Cl_2. The extract was washed with water and the combined organic phases were dried over Na_2SO_4. **TPA-T-C6-Sn** (2.50 g, 91%) was obtained as brown oil and used in the next reaction without further purification.

BTT-T

5,8-Dibromodithieno[3',2':3,4;2",3":5,6]benzo[1,2-c][1,2,5]thiadiazole was synthesized according to literature.[4]

5,8-Dibromodithieno[3',2':3,4;2",3":5,6]benzo[1,2-c][1,2,5]thiadiazole (0.50 g, 1.23 mmol), **TPA-T-C6-Sn** (2.06 g, 2.71 mmol) and $Pd(PPh_3)_4$ (142.27 mg, 0.12 mmol) were placed in a round-bottomed flask. Toluene (10 mL, degassed with nitrogen) was added. The mixture was refluxed for 48 h. After cooling to room temperature, the mixed solution was extracted with CH_2Cl_2, washed with water, dried and evaporated under vacuum. **BTT-T** (1.21 g, 83%) was obtained by column chromatography on silica gel

using petroleum ether/ethyl acetate, 4:1, v/v. ^{1}H NMR (500 MHz, $CDCl_3$, δ): 7.98 (s, 2H), 7.27 (s, 4H), 7.21 (s, 4H), 7.10 (s, 6H), 6.87 (s, 12H), 3.82 (s, 12H), 2.67 (s, 4H), 1.73 – 1.59 (m, 4H), 1.40 – 1.24 (m, 12H), 0.90 (t, J = 6.4 Hz, 6H). ^{13}C NMR (125 MHz, $CDCl_3$, δ): 156.14, 150.18, 148.28, 140.54, 138.97, 138.92, 137.59, 133.23, 133.15, 129.59, 129.39, 127.53, 126.95, 125.54, 119.66, 118.76, 114.79, 55.49, 31.68, 30.92, 29.28, 28.93, 22.64, 14.14. MALDI-TOF MS: m/z=1186.3673 $[M]^+$, calcd. for $C_{70}H_{66}N_4O_4S_5$: 1186.3688. Elemental analysis: calcd. for $C_{70}H_{66}N_4O_4S_5$: C 70.79, H 5.60, N 4.72, S 13.50; found: C 70.09, H 5.54, N 4.49, S 13.87.

3. Device fabrication

Solution preparation:

$MA_{0.7}FA_{0.3}PbI_3$ precursor: 1 mmol PbI_2 (Alfa Aesar), 0.7 mmol methylammonium iodide (MAI, Dyesol), 0.3 mmol formamidinium iodide (FAI, Dyesol) and 9.22 mg $Pb(SCN)_2$ (Sigma-Aldrich, 99.5%) were added to 600 μL *N*,*N*-dimethylformamide (DMF, Sigma-Aldrich), then 1 mmol dimethyl sulfoxide (DMSO, Sigma-Aldrich) was added. The precursor solution was stirred on a hotplate at 60 ℃ for 1 h and then purified using a 0.45 μm filter before deposition.

C_{60}-SAM: C_{60}-SAM (Sigma-Aldrich, 99.8%) was dissolved in chlorobenzene (CB)with a concentration of 4 mg mL^{-1}.

PEAI: A solution of PEAI (2 mg mL^{-1} in isopropanol, Sigma Aldrich) was purified using a 0.45 μm filter before deposition.

BDD-T/BTT-T: A solution of BDD-T/BTT-T (15 mg mL^{-1} in CB) was stirred on a hotplate at 50 ℃ for 1 h and then purified using a 0.45 μm filter before deposition.

Spiro-OMeTAD: The spiro-OMeTAD solution was prepared by dissolving 72.3 mg spiro-OMeTAD (Shenzhen Feiming Science and Technology Co., Ltd.) in 1 mL CB with 28 μL *t*-BP (Sigma-Aldrich) and 18 μL Li-TFSI (520 mg mL^{-1} in acetonitrile, Sigma-Aldrich). The solution was stirred on a hotplate at 60 ℃ for 24 h and then purified using a 0.45 μm filter before deposition.

Device fabrication:

The FTO substrates were sequentially cleaned by ultra-sonication with diluted Micro-90 detergent, deionized water, acetone, and isopropanol for 30 min, respectively. SnO_2 layer was deposited on the FTO from a pre-synthesized QD solution.[5] The SnO_2 layer was annealed at 200 ℃ for 1 h in imbient air. The C_{60}-SAM solution was then spin-coated onto SnO_2 layer at 3000 rpm for 1 min. The perovskite precursor solution was

spin-coated at 500 rpm for 3 s and at 4000 rpm for 60 s, 700 μL diethyl ether was then dropped onto the perovskite surface at 55s before end in one portion. After spin-coating, the perovskite film was annealed at 100 ℃ for 5 min. All these processes were carried out in a N_2 filled glove box. The PEAI layer was spin-coated on the top of the perovskite film at a speed of 5000 rpm for 30 s. The HTM layer was spin-coated on the perovskite film at 3000 rpm for 60 s. All HTM films are fabricated without thermal annealing. A layer of 100 nm gold (Au) was then deposited on the top of HTM using thermal evaporation. The working area of the devices was 0.04 cm^2 as defined by a shadow mask during the Au evaporation.

4. ^{1}H NMR, ^{13}C NMR and MALDI-TOF MS spectra

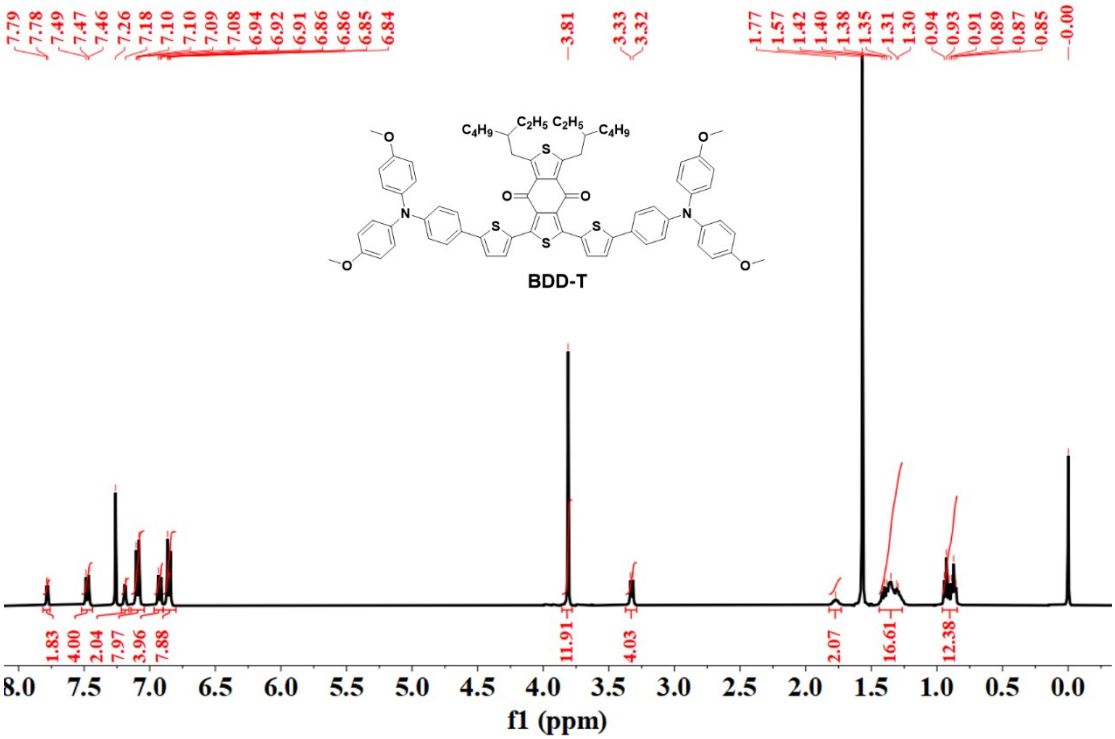

Fig. S1 ^{1}H NMR spectrum of compound **BDD-T**.

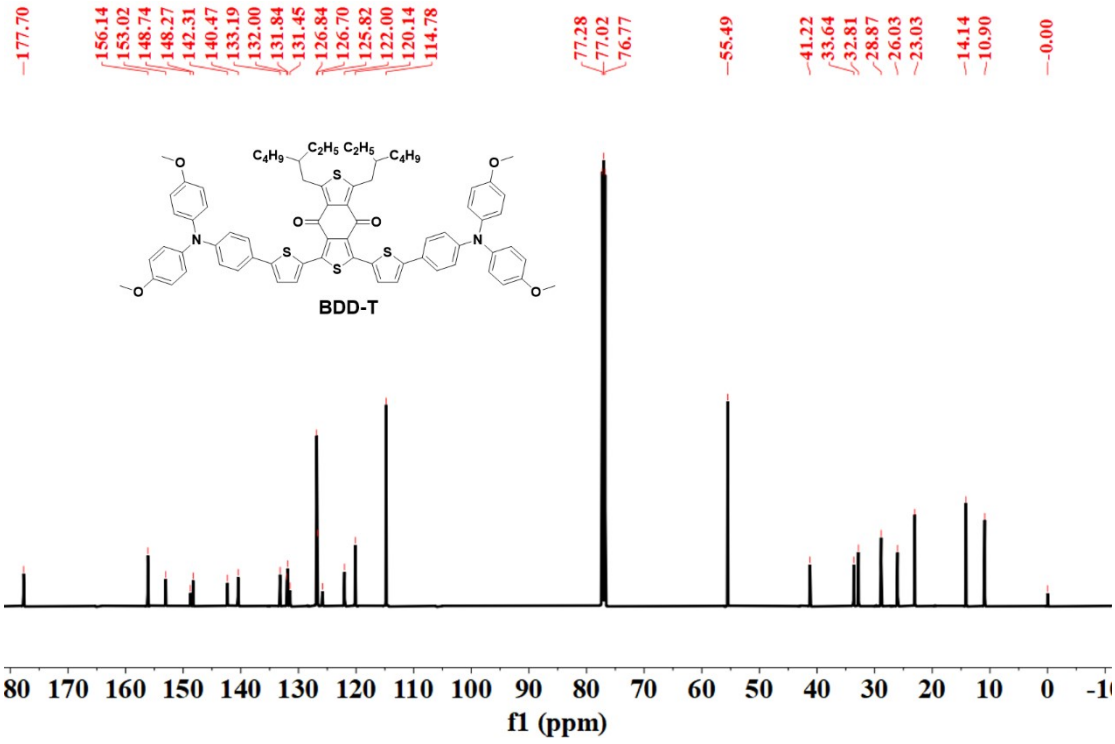

Fig. S2 ^{13}C NMR spectrum of compound **BDD-T**.

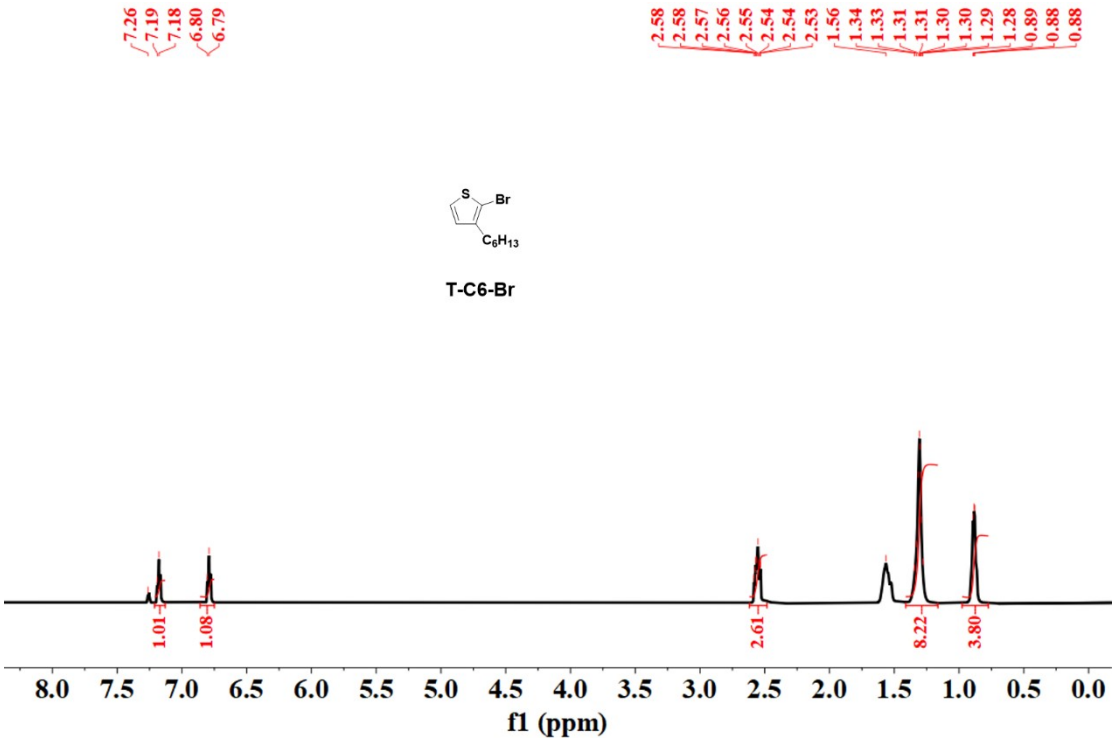

Fig. S3 ^{1}H NMR spectrum of compound **T-C6Br**.

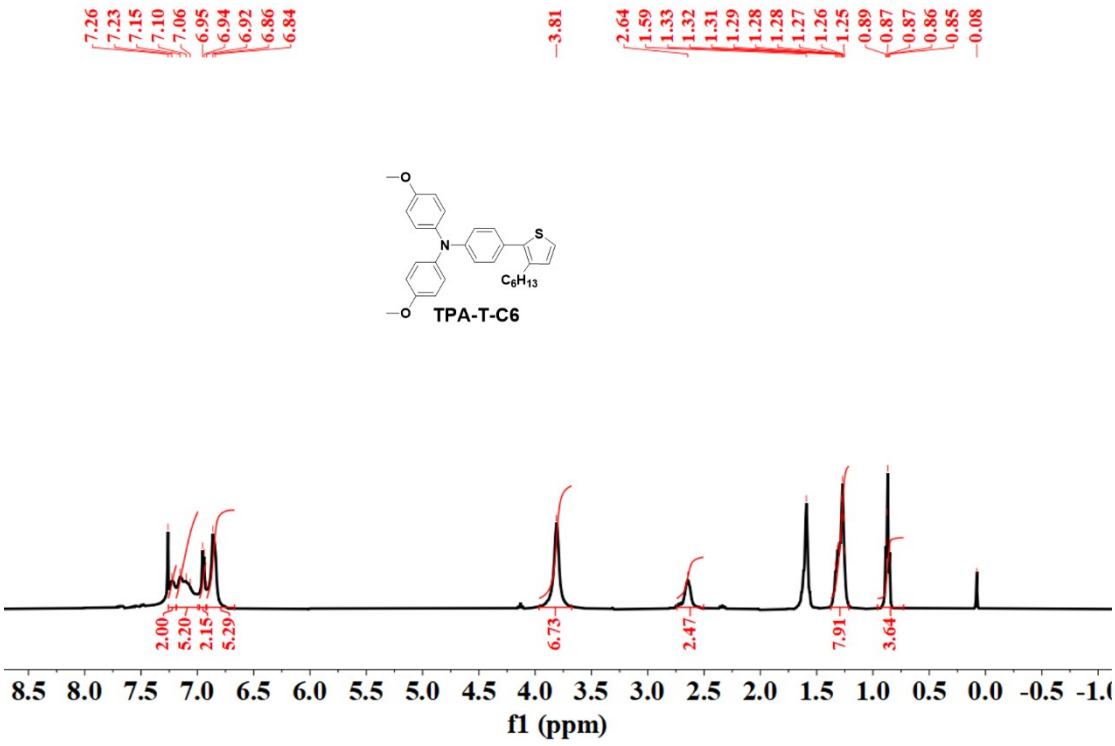

Fig. S4 [1]H NMR spectrum of compound **TPA-T-C6**.

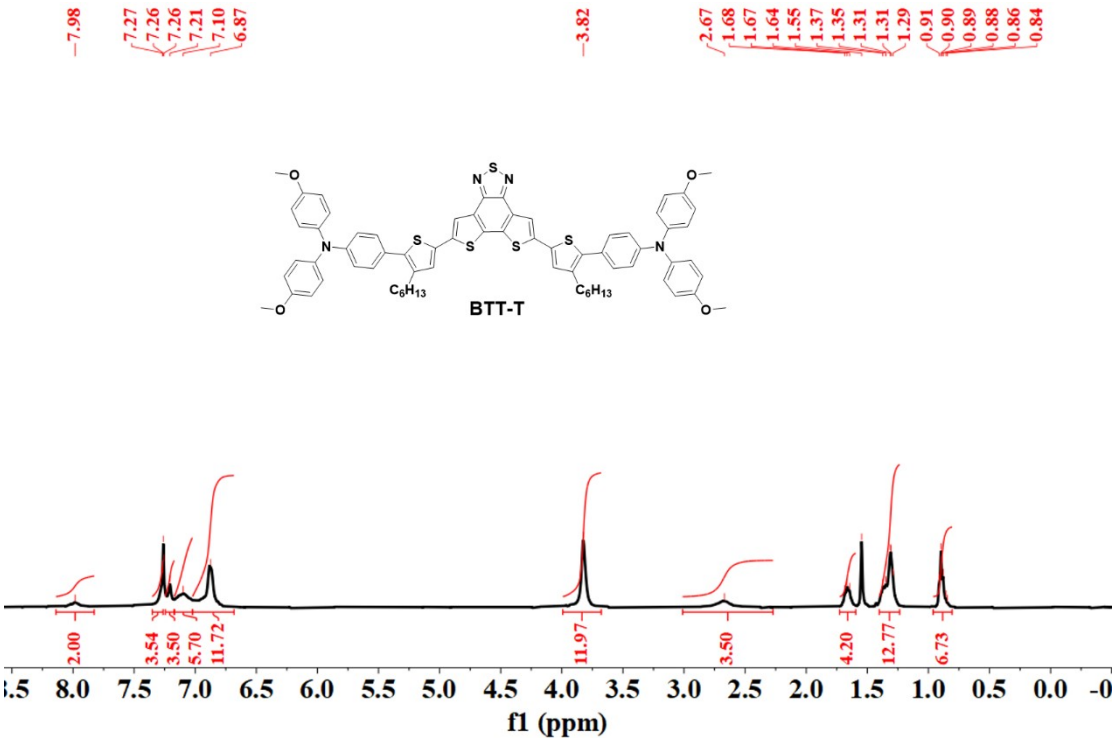

Fig. S5 [1]H NMR spectrum of compound **BTT-T**.

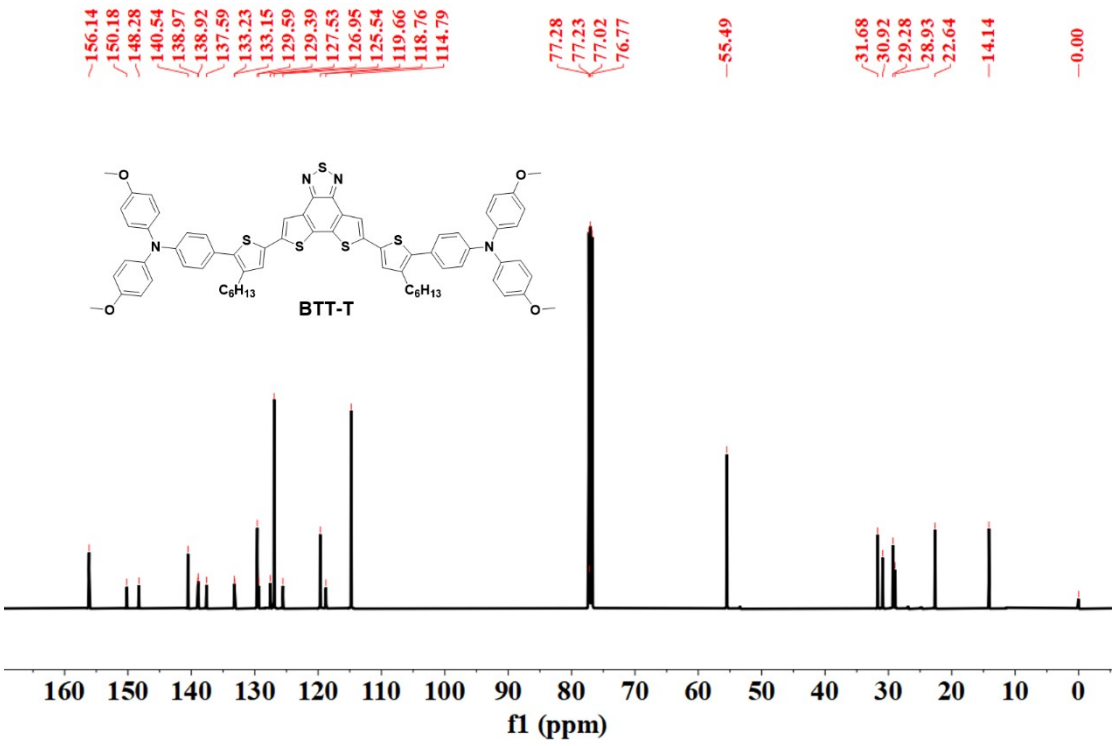

Fig. S6 ^{13}C NMR spectrum of compound **BTT-T**.

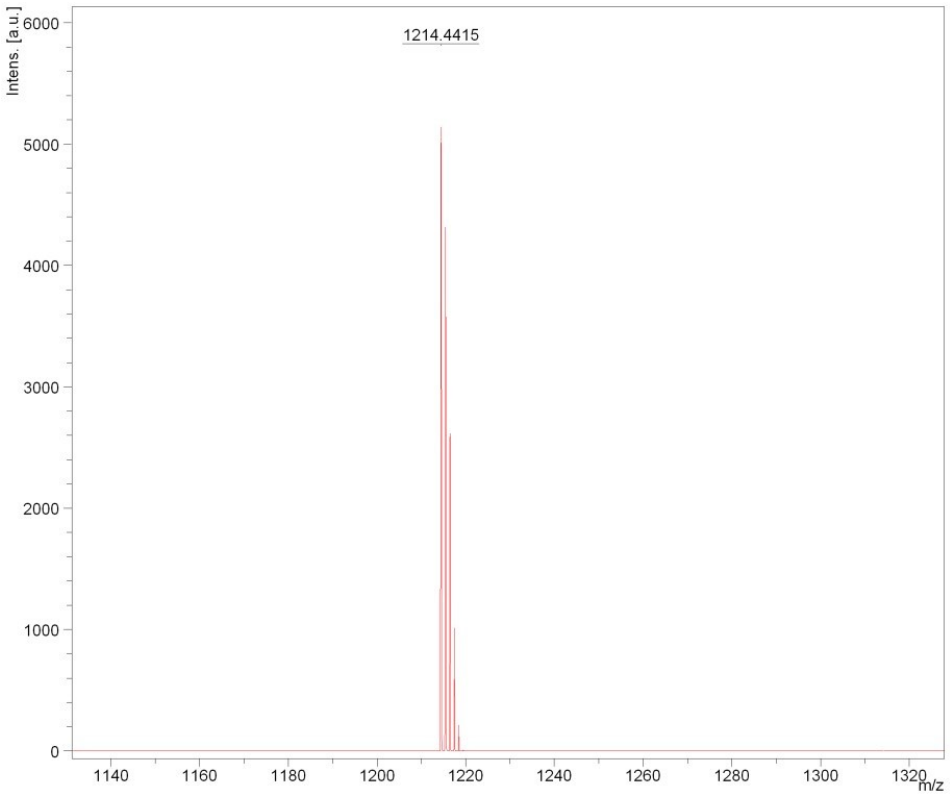

Fig. S7 MADLI-TOF mass spectrometry of **BDD-T**.

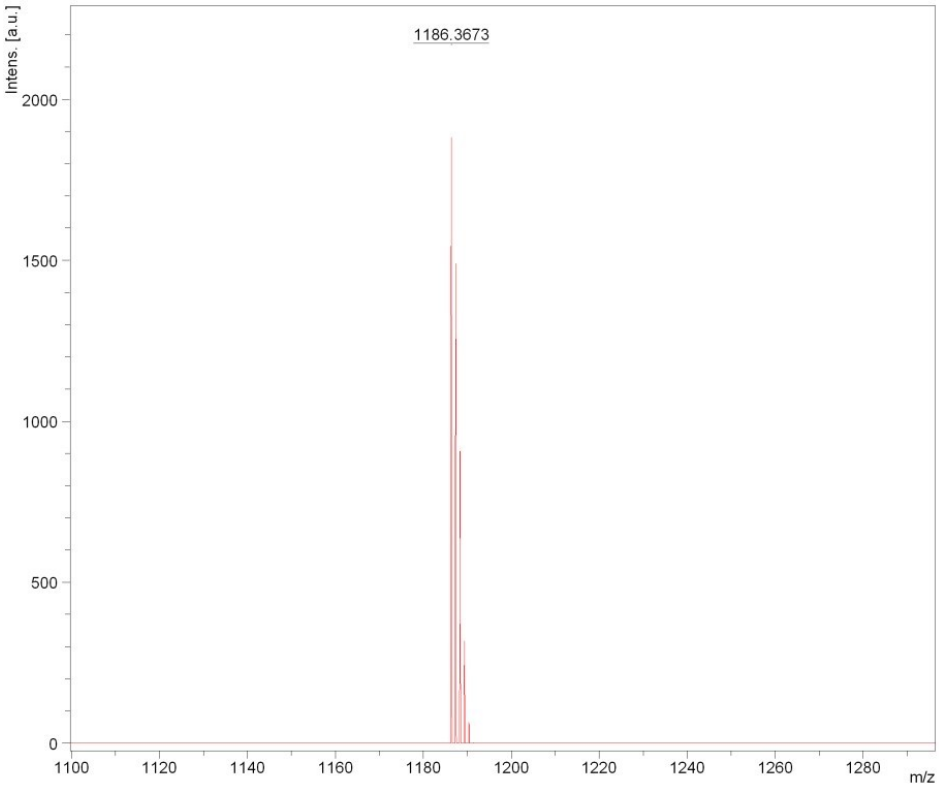

Fig. S8 MADLI-TOF mass spectrometry of **BTT-T**.

5. DFT calculation

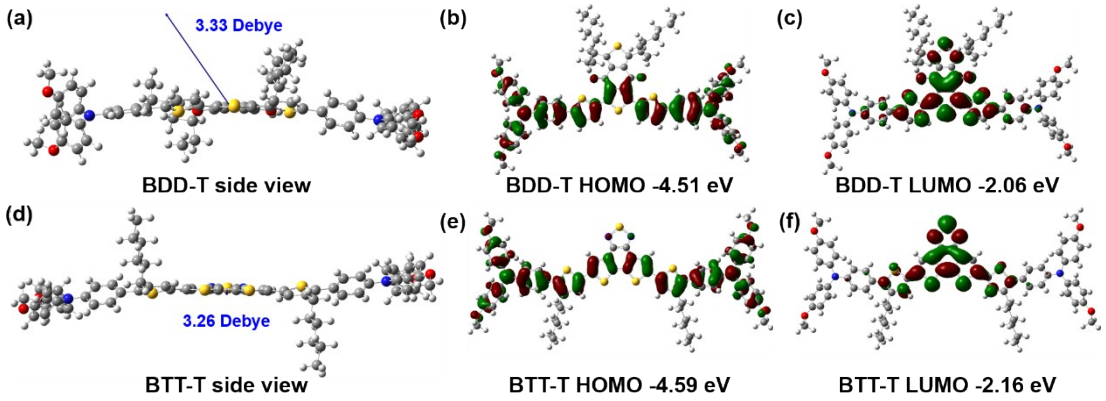

Fig. S9 DFT calculated geometries and frontier orbitals of BDD-T: (a) side view geometry and total dipole moment, (b) HOMO and (b) LUMO delocalization. DFT calculated geometries and frontier orbitals of BTT-T: (d) side view geometry and total dipole moment, (e) HOMO and (f) LUMO delocalization.

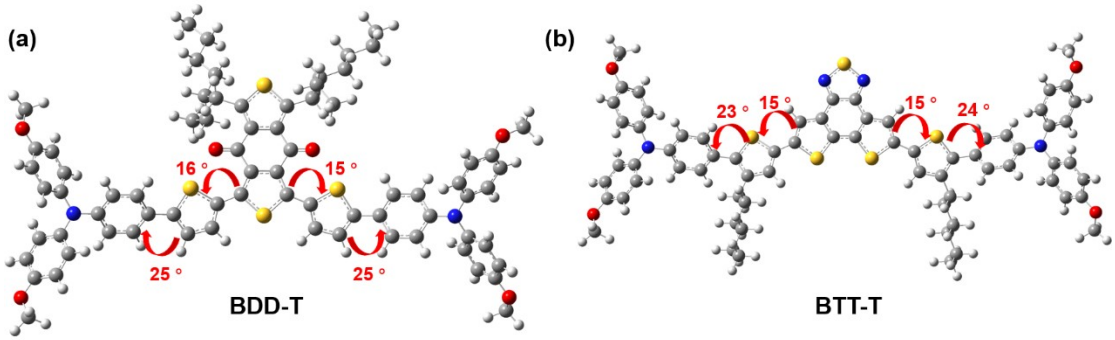

Fig. S10 DFT calculated geometries (top view) and dihedral angles of (a) BDD-T and (b) BTT-T.

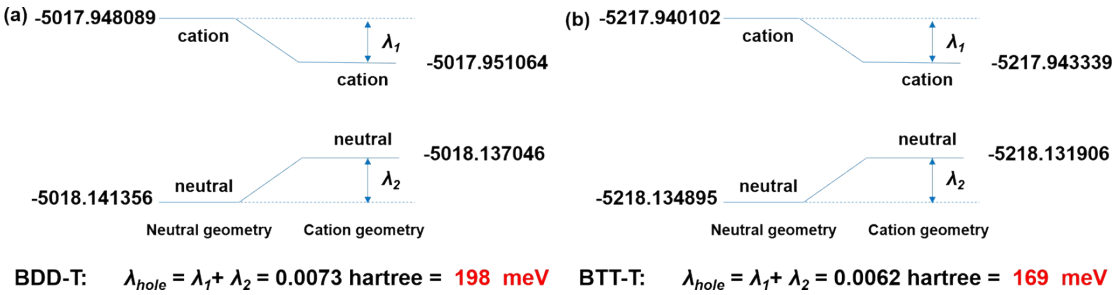

Fig. S11 DFT calculated hole reorganization energies of (a) BDD-T and (b) BTT-T.

6. CV, AFM, SEM and water contact angle results

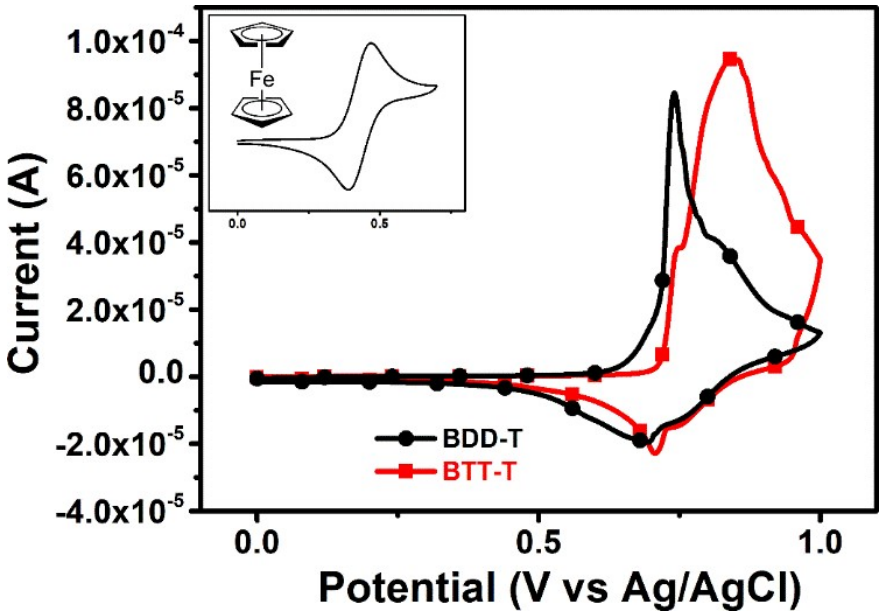

Fig. S12 CV plots of BDD-T and BTT-T. The inset is the CV plot of ferrocene/ferrocenium standard.

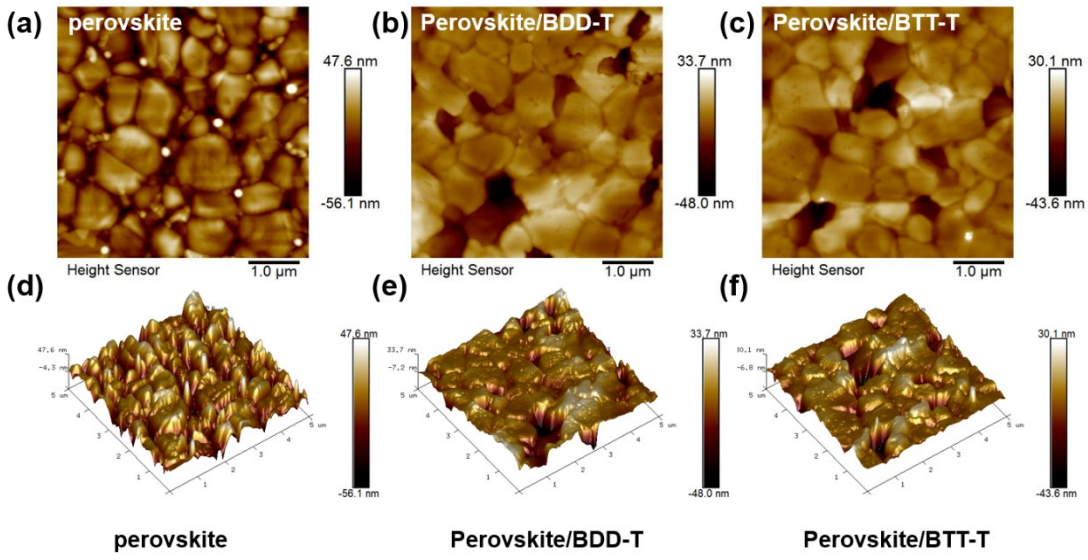

Fig. S13 AFM 2D images of (a) bare perovskite and perovskite covered with (b) BDD-T and (c) BTT-T films. AFM 3D images of (d) bare perovskite and perovskite covered with (e) BDD-T and (f) BTT-T films. The surface roughness with root-mean-square (RMS) of perovskite, perovskite/BDD-T and perovskite/BTT-T are 14.6, 10.2 and 8.7 nm, respectively.

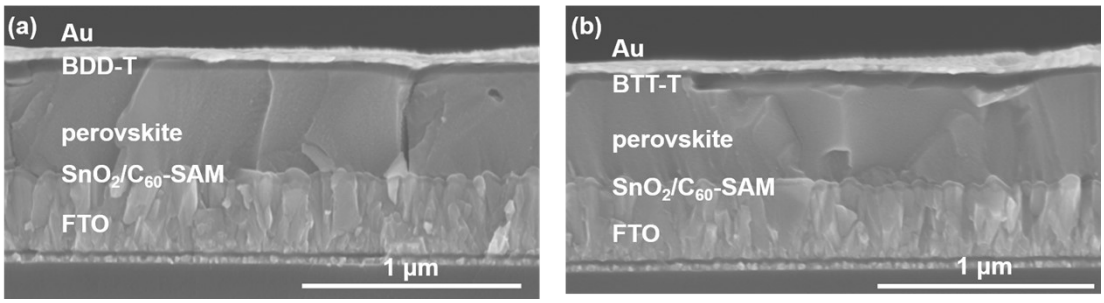

Fig. S14 Cross-sectional SEM image of PSCs with (a) BDD-T and (b) BTT-T HTMs. The estimated thicknesses of BDD-T and BTT-T are 57 and 62 nm.

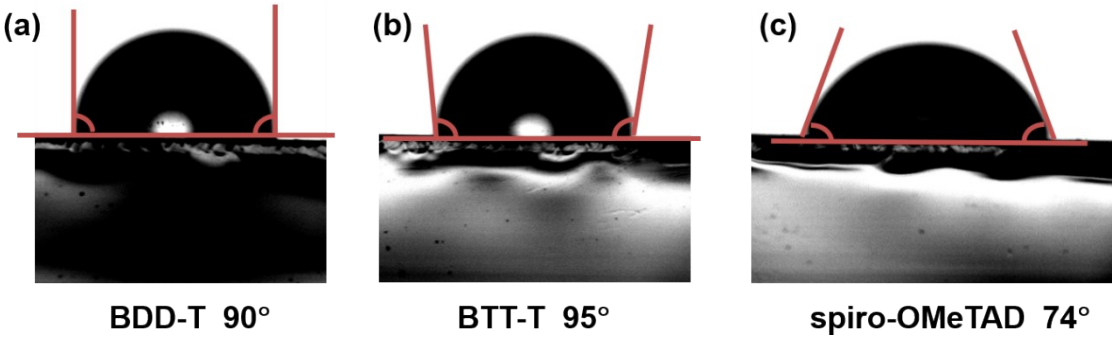

Fig. S15 Water contact angles of perovskite covered with (a) BDD-T, (b) BTT-T and (c) doped spiro-OMeTAD films.

7. Device parameters

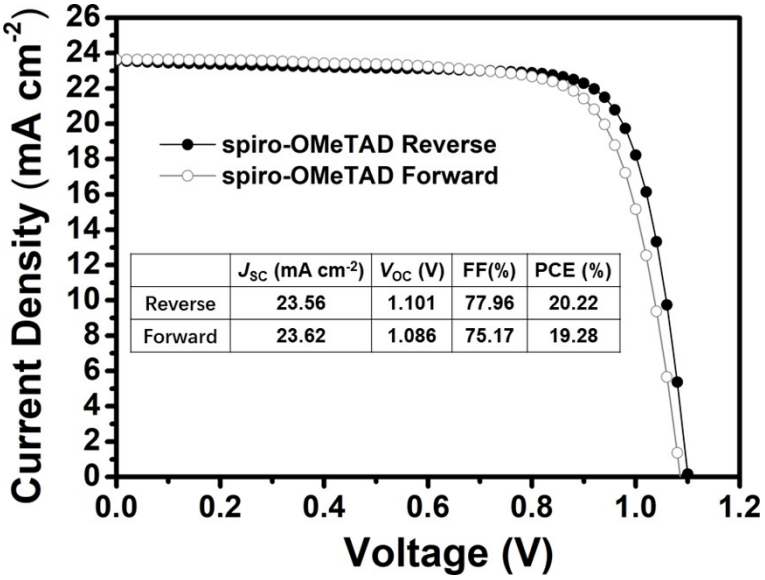

	J_{SC} (mA cm^{-2})	V_{OC} (V)	FF(%)	PCE (%)
Reverse	23.56	1.101	77.96	20.22
Forward	23.62	1.086	75.17	19.28

Fig. S16 *J-V* curves of doped spiro-OMeTAD-based PSCs measured under reverse and forward voltage scan. The inset is the summary of photovoltaic parameters.

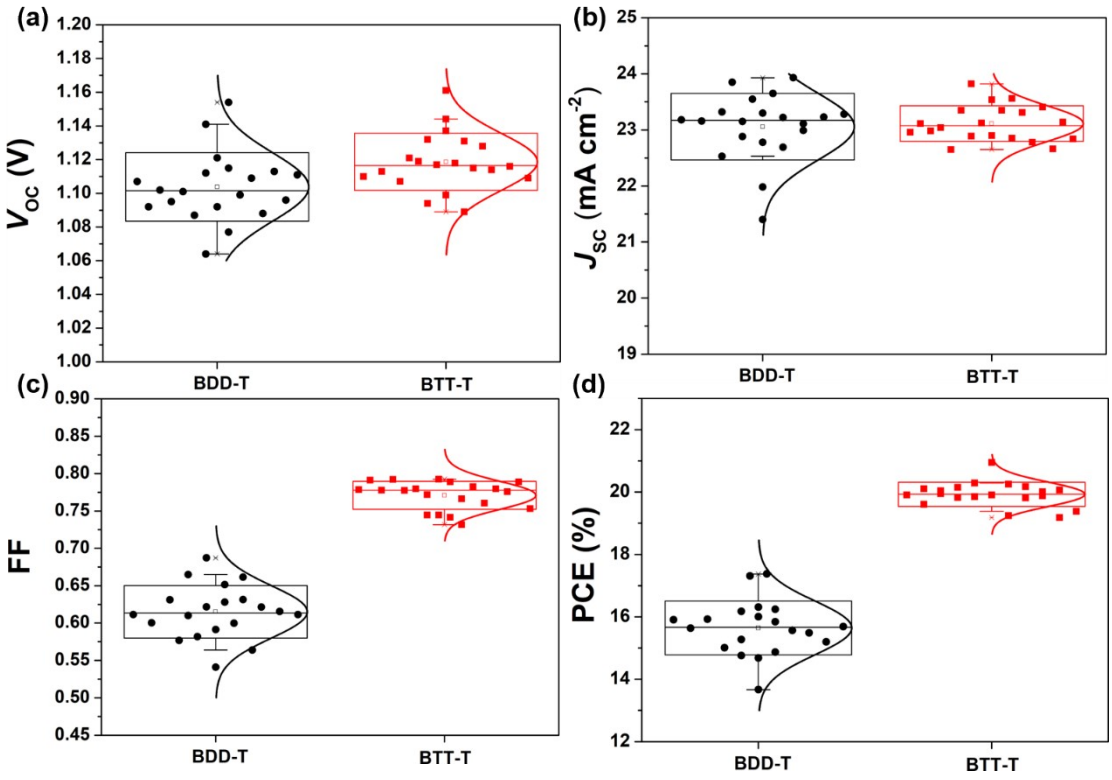

Fig. S17 Photovoltaic parameters of 20 individual PSCs with BDD-T and BTT-T as HTMs. Histograms of (a) V_{OC}, (b) J_{SC}, (c) FF, and (d) PCE of corresponding devices.

Table S1 Photovoltaic parameters for PSCs with BDD-T and BTT-T as HTMs.

HTM	J_{SC} (mA cm^{-2})	V_{OC} (V)	FF	PCE (%)
BDD-T	23.06±0.24	1.104±0.011	0.6150±0.0129	15.64±0.67
BDD-T champion	23.30	1.115	0.6279	16.31
BTT-T	23.11±0.24	1.119±0.018	0.7709±0.0180	19.93±1.01
BTT-T champion	23.35	1.137	0.7889	20.94

8. A summary of representative D-A-D type HTMs

Table S2 A summary of representative D-A-D type HTMs for n-i-p PSCs.

HTM	Dopant-free	J_{SC} (mA cm^{-2})	V_{OC} (V)	FF	PCE (%)	Ref.
BTT-T	**Yes**	**23.35**	**1.137**	**0.7889**	**20.94**	**This work**
Y-T	Yes	22.90	1.118	0.7925	20.29	[6]
YN2	Yes	22.87	1.11	0.75	19.27	[7]
TQ4	Yes	23.71	1.124	0.79	21.03	[8]
BTF4	Yes	22.5	1.06	0.756	18.03	[9]
FBA3	Yes	22.12	1.09	0.799	19.27	[10]
DT-BT	Yes	16.8	0.83	0.522	7.3	[11]
ACE-QA-ACE	Yes	22.41	1.06	0.77	18.2	[12]
TQ2	No	22.55	1.12	0.7767	19.62	[13]
JY6	No	21.39	1.066	0.81	18.54	[14]
JY8	No	21.94	1.08	0.81	19.14	[15]

9. References

1. L. Guan, X. Yin, D. Zhao, C. Wang, Q. An, J. Yu, N. Shrestha, C. Grice, R. Awni, Y. Yu, Z. Song, J. Zhou, W. Meng, F. Zhang, R. Ellingson, J. Wang, W. Tang and Y. Yan, *J. Mater. Chem. A*, 2017, **5**, 23319-23327.
2. D. Qian, L. Ye, M. Zhang, Y. Liang, L. Li, Y. Huang, X. Guo, S. Zhang, Z. a. Tan and J. Hou, *Macromolecules*, 2012, **45**, 9611-9617.
3. X. Yin, L. Guan, J. Yu, D. Zhao, C. Wang, N. Shrestha, Y. Han, Q. An, J. Zhou, B. Zhou, Y. Yu, C. R. Grice, R. A. Awni, F. Zhang, J. Wang, R. J. Ellingson, Y. Yan and W. Tang, *Nano Energy*, 2017, **40**, 163-169.
4. J. Lee, D. H. Sin, J. A. Clement, C. Kulshreshtha, H. G. Kim, E. Song, J. Shin, H. Hwang and K. Cho, *Macromolecules*, 2016, **49**, 9358-9370.
5. G. Yang, C. Chen, F. Yao, Z. Chen, Q. Zhang, X. Zheng, J. Ma, H. Lei, P. Qin, L. Xiong, W. Ke, G. Li, Y. Yan and G. Fang, *Adv. Mater.*, 2018, **30**, 1706023.
6. J. Hai, H. Wu, X. Yin, J. Song, L. Hu, Y. Jin, L. Li, Z. Su, Z. Xu, H. Wang and Z. Li, *Adv. Funct. Mater.*, 2021, **31**, 2105458.
7. P. Xu, P. Liu, Y. Li, B. Xu, L. Kloo, L. Sun and Y. Hua, *ACS Appl. Mater. Interfaces*, 2018, **10**, 19697-

19703.

8. H. Guo, H. Zhang, C. Shen, D. Zhang, S. Liu, Y. Wu and W.-H. Zhu, *Angew. Chem., Int. Ed.*, 2021, **60**, 2674-2679.
9. X. Sun, Q. Xue, Z. Zhu, Q. Xiao, K. Jiang, H.-L. Yip, H. Yan and Z. a. Li, *Chem. Sci.*, 2018, **9**, 2698-2704.
10. X. Sun, F. Wu, C. Zhong, L. Zhu and Z. a. Li, *Chem. Sci.*, 2019, **10**, 6899-6907.
11. T. Niu, W. Zhu, Y. Zhang, Q. Xue, X. Jiao, Z. Wang, Y.-M. Xie, P. Li, R. Chen, F. Huang, Y. Li, H.-L. Yip and Y. Cao, *Joule*, 2021, **5**, 249-269.
12. H. D. Pham, S. M. Jain, M. Li, S. Manzhos, K. Feron, S. Pitchaimuthu, Z. Liu, N. Motta, H. Wang, J. R. Durrant and P. Sonar, *J. Mater. Chem. A*, 2019, **7**, 5315-5323.
13. H. Zhang, Y. Wu, W. Zhang, E. Li, C. Shen, H. Jiang, H. Tian and W. Zhu, *Chem. Sci.*, 2018, **9**, 5919-5928.
14. F. Wu, Y. Ji, C. Zhong, Y. Liu, L. Tan and L. Zhu, *Chem. Commun.*, 2017, **53**, 8719-8722.
15. Y. Ji, B. He, H. Lu, J. Xu, R. Wang, Y. Jin, C. Zhong, Y. Shan, F. Wu and L. Zhu, *ChemSusChem*, 2019, **12**, 1374-1380.